EI SEVIER

Contents lists available at ScienceDirect

Journal of Sound and Vibration

journal homepage: www.elsevier.com/locate/jsvi



Active cloaking of flexural waves in thin plates



Gregory Futhazar a, William J. Parnell b,*, Andrew N. Norris c

- ^a IRMAR, Université Rennes 1, 263 avenue du Général Leclerc, CS 74205, 35042 Rennes Cédex, France
- ^b School of Mathematics, University of Manchester, Oxford Road, Manchester M13 9PL, UK
- ^c Mechanical and Aerospace Engineering, Rutgers University, Piscataway, NJ 08854-8058, USA

ARTICLE INFO

Article history:
Received 12 August 2014
Received in revised form
6 May 2015
Accepted 11 June 2015
Handling Editor: M.P. Cartmell
Available online 23 July 2015

ABSTRACT

An active cloak consists of a set of discrete multipole sources distributed in space. When the source positions and amplitudes are carefully specified the active field destructively interferes with an incident time harmonic wave so as to nullify the total field in some finite domain and ensure that in the far field only the incident wave is present, i.e. the active field is non-radiating. Here it is shown how to efficiently determine the source coefficients explicitly in the context of flexural waves in thin plates. The work is carried out in the context of Kirchhoff plate theory, using the Rayleigh–Green theorem to derive the unique source amplitudes for a given incident flexural wave.

© 2015 The Authors. Published by Elsevier Ltd. This is an open access article under the CC BY license (http://creativecommons.org/licenses/by/4.0/).

1. Introduction

Controlling and limiting the vibration of thin plates has a multitude of applications in structural acoustics. It is a subject that has received great attention in the literature where a variety of techniques have been proposed to reduce the level of structural vibration and noise. See for example [1], the text by Fuller et al. [2] and for an early example see e.g. Olson [3]. A closely related topic that has emerged over the last decade is that of cloaking, the effect of causing a region to be unseen by incoming waves in the sense that the scattering is zero in all directions, see [4] for a review. Two principal techniques have been proposed: passive and active. Passive cloaking [5–7] requires complex metamaterials in order to guide waves around some volume of space, or around a region in a plate. Passive cloaking methods have been successfully developed and demonstrated for flexural waves in thin plates. Thus, Stenger et al. [8] adapted the design proposed in [9] to make a free-space flexural wave cloak in a thin PVC plate. The flexural wave cloak was demonstrated at acoustic frequencies, and exhibited the largest measured relative bandwidth (more than one octave) of reported free-space acoustic cloaks.

In contrast to passive methods, *active cloaking* uses sources of sound to achieve wave cancellation. It does not involve or call for unusual materials or structural modifications. Active cloaking does however require knowledge of the incident field in order to activate wave sources that nullify the total field in a given region. Importantly the sources must be non-radiating.

Miller [10] first proposed the notion of actively cloaking a region by measuring particle motion near the surface of the cloaked zone while simultaneously exciting surface sources where each source amplitude depends on the measurements at all sensing points. Complete suppression of sound in a finite volume in an unbounded domain can be achieved using a continuous distribution of monopoles and dipoles with source amplitudes given by the Kirchhoff–Helmholtz integral formula [11]. The main disadvantage of solutions based on the Kirchhoff–Helmholtz integral is the difficulty of realizing in practice acoustically transparent sensor and actuator surfaces. It would be better to replace the surfaces by finite sets of discrete sensors and

E-mail addresses: gregory.futhazar@gmail.com (G. Futhazar), william.parnell@manchester.ac.uk (W.J. Parnell), norris@rutgers.edu (A.N. Norris).

^{*} Corresponding author. Tel.: $+44\ 161\ 275\ 5908$.

sources. As an active cloaking method this approach is also limited because it does not provide a unique relationship between the incident field and the source amplitudes. A solution to this problem was provided by Guevara Vasquez et al. [12–14] who showed that cloaking can be realized using as few as three active sources in 2D and four in 3D, a remarkable result. In [12,13] algebraic systems were solved numerically to determine the required active source coefficients. Recently however explicit forms for the source amplitudes in terms of the incident wave were derived in the contexts of scalar Helmholtz [15] and elastodynamics [16], both in two dimensions. The sources required in these solutions are multipoles, and full cloaking needs multipoles of all order. Such infinite multipole expansions are divergent, a point that was noted in the anti-sound community [11, pp. 262–4]. In practice, the infinite series is truncated, which limits accuracy but numerical simulations indicate that only a small number of multipoles may be required [15]. Despite such limitations, these results provide a rigorous basis for subsequent approximation. Other approaches to active cloaking have been suggested; for instance, Bobrovnitskii [17] described an active impedance-matching solution to making an object acoustically transparent, and also summarized earlier relevant work by Malyuzhinets. Bobrovnitskii later proposed acoustic cloaking using a non-local impedance coating, called coatings with extended reaction (CER) [18].

Active cloaking is closely related to active noise control and *anti-sound*, the notion of which appears to have been considered first in a patent published in 1936 by Paul Lueg [19]. The focus of anti-sound or anti-vibration is to reduce the magnitude of a radiating field or to create so-called quiet zones in enclosed domains such as aircraft cabins using simple sources, see e.g. [20] for an overview. Typically a continuous distribution of monopoles and dipoles is employed as described in [2,11], although in practice only a finite number can be used. The difficulty in going from the former to the latter has been discussed many times, see e.g. [21]. No conditions are placed on the active field other than that it must nullify some field over a finite domain and in particular it is permitted to radiate into the far field. This is in contrast to active cloaking described here where the active field must not radiate. Relatively little work in the anti-sound community has focused on the exact shape of the quiet zone with the exception of [22] who calculated numerically the zone of silence (< 10 dB) region created when the amplitude of a single secondary source was chosen to reduce noise due to a single primary source.

The purpose of this paper is to develop exact solutions for active cloaking of flexural waves in plates. The present work adapts the method employed in [15,16] to achieve active cloaking in thin plates of uniform thickness and of infinite extent. The problem is considered in the context of the Kirchhoff plate theory, an approximate theory requiring that the plate thickness h is small compared to other characteristic length scales, but not so thin that the lateral deflection of the plate is comparable to h. Kirchhoff theory is notable in that shear energy is neglected and there is uncoupled membrane-bending action. Improvements to the theory can, of course, be considered but the Kirchhoff theory is extremely accurate in many physical applications in structural acoustics. The analysis presented here was first detailed in the PhD thesis of Futhazar [23].

A procedure for active cloaking in flexural plates proposed by [24] differs significantly from the present work in that the authors choose a fixed number of active sources and then determine the monopole coefficients required to nullify a certain number of modal amplitudes from the scattered field. The method developed here is precise in principle, relying on the use of multipoles with amplitude uniquely and directly specified by the incident wave field.

The outline of the paper is as follows. Section 2 begins with an overview of the problem to be discussed and a brief review of Kirchhoff plate theory. The relevant integral relation is derived in Section 3, from which the main results regarding the explicit form of the source amplitudes and cloaked domain are shown to follow. General forms for the coefficients are derived and specific results derived for plane wave and point source incidence follow. In Section 4 necessary and sufficient conditions on the source coefficients are derived in order to ensure active cloaking. Numerical results to illustrate the implementation of the procedure for plane wave incidence follow in Section 5.

2. Kirchhoff thin plate theory and problem overview

With reference to Fig. 1, the aim is to control the vibration of thin plates via M idealized point sources and in particular to nullify an incident field in some finite region \mathcal{C} . The domain \mathcal{C} is usually close to the source locations and in addition, unlike the case of anti-vibration, the aim is to ensure that the active field is non-radiating so that no evidence exists of its presence. If this can be achieved an active cloak has been constructed. In this paper the assumption is that vibrations are small enough

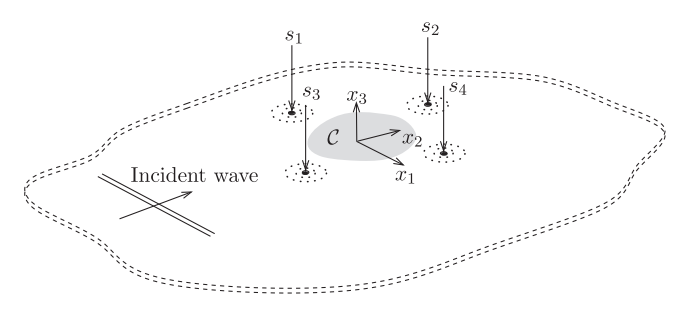


Fig. 1. An incident flexural wave is illustrated propagating in a thin plate that is unbounded in the x_1x_2 plane. The aim of active cloaking in this context is to nullify the total flexural vibration of the plate in some finite region \mathcal{C} by employing active sources, $s_1 - s_4$ here, whilst simultaneously ensuring that the radiated field due to the active sources is zero.

so that the Kirchhoff theory accurately describes their propagation and the forcing required to activate each active source itself does not cause scattering of any incident field. The Kirchhoff theory will first be summarized before explicit forms for the amplitudes of the multipole active cloak are derived.

2.1. Kirchhoff thin plate theory

As depicted in Fig. 1 consider a thin plate that is unbounded in the x_1x_2 plane. Its thickness is h and is considered small compared to other length scales of the problem but large compared to the amplitude of the flexural vibration. As such, Kirchhoff theory is appropriate to accurately describe its deformation [25]. The plate properties are density ρ and flexural rigidity $D = Eh^3/(12(1-\nu^2))$ where E and ν are Young's modulus and Poisson's ratio. The axes x_1 and x_2 of the Cartesian reference system ($\mathbf{0}, x_1, x_2, x_3$) lie on the middle plane of the plate whereas x_3 is the out-of-plane (vertical) coordinate. The out-of-plane displacement is denoted $W(\mathbf{x}, t)$ where \mathbf{x} is defined as $\mathbf{x} = (x_1, x_2)$. The equation of motion governing the flexural deflection is

$$D\nabla^2\nabla^2W + \rho h \frac{\partial^2W}{\partial t^2} = f \tag{1}$$

where f is the applied loading (force per unit area). Assume time harmonic behaviour, $W(\mathbf{x},t) = \text{Re}\{w(\mathbf{x})e^{-i\omega t}\}$ where ω is the angular frequency so that

$$D(\nabla^2 \nabla^2 - k^4) w = D(\nabla^2 + k^2)(\nabla^2 - k^2) w = f$$
 (2)

where the wavenumber k is defined by $k^4 = \omega^2 \rho h/D$. The total field will be partitioned as

$$w(\mathbf{x}) = \tilde{w}(\mathbf{x}) + w_d(\mathbf{x}) \tag{3}$$

where \tilde{w} is the specified incident field and w_d is the non-radiating active field. In the next section the problem is formulated in detail and appropriate expansions of the wave fields \tilde{w} and w_d are specified. In the section to follow the desired amplitudes of the various modes in the expansions associated with the active field are then derived exactly using the Rayleigh–Green theorem and thus the active cloak is constructed.

2.2. An overview of the active cloaking problem

The active cloaking system considered here consists of an array of M point-like multipole sources located at positions $\mathbf{x}_m \in \mathbb{R}^2$ for $m \in \{1, ..., M\}$. The amplitude of the individual active sources is required to be of a form such that the incident field is nullified by destructive interference in some finite domain \mathcal{C} . Defects and inhomogeneities in the region \mathcal{C} therefore do not scatter and are undetectable by an incoming wave. The total active field w_d must also be non-radiating. The active sources are in the exterior region with respect to \mathcal{C} and this type of cloaking is therefore termed active exterior cloaking. As identified previously [15,16], the advantages of this cloaking mechanism are that

- the cloaked region is not completely surrounded by a single cloaking device,
- a small number of active sources are required,
- the procedure works in principle for broadband input sources,
- the cloaking effect is independent of the location of the scatterer or scatterers in the cloaked region.

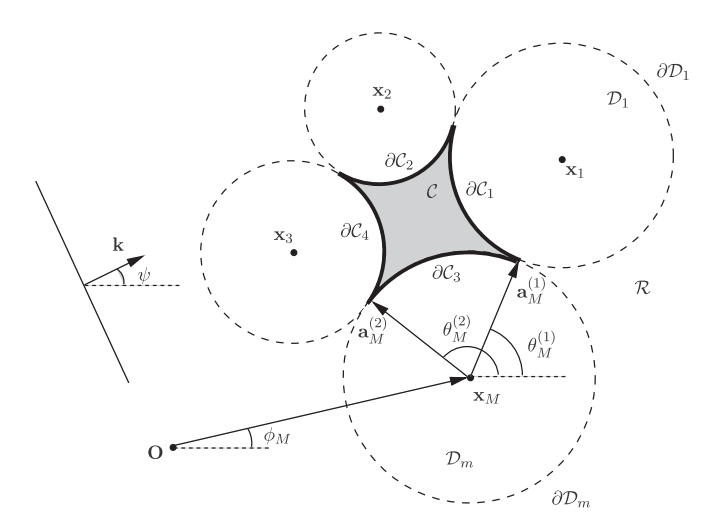


Fig. 2. Insonification of the actively cloaked region $\mathcal C$ generated by M active sources at $\mathbf x_m$, $m \in \{1, ..., M\}$. The region $\mathcal R$ is defined as the exterior to the dashed circular arcs $\partial \mathcal D_i$, i=1,2,...,M. The incident field in this case is a plane wave vector $\mathbf k$ in the direction ψ . Here $\mathbf a_m^{(i)} = a_m \hat{\mathbf e}(\theta_m^{(i)})$ where $\hat{\mathbf e}(\theta)$ is a unit vector subtended at an angle θ from the horizontal.

A disadvantage of this approach is that the active field may become uncontrollably large in the vicinity of the (point) source positions. Realistically such sources would be of finite extent however and as such the resulting magnitude of the field would be significantly reduced. It must also be stressed that the incident field must be known. Nevertheless it is emphasized that all that is required is an expansion of the incident field in the same basis as the active field, to be specified shortly in (4).

The technique is illustrated in Fig. 2 where \mathcal{C} depicts the cloaked zone generated by M active sources. It is shown in Section 3.2 that the boundary of \mathcal{C} is the closed union of the M circular arcs $\{a_m, \theta_m^{(1)}, \theta_m^{(2)}\}$ related to the sources at \mathbf{x}_m . Circular arcs arise as a consequence of Graf's addition theorem. In the general case $a_m, \theta_m^{(1)}$ and $\theta_m^{(2)}$ are distinct for different values of m. Fig. 2 illustrates the problem in the context of plane-wave incidence but expressions for source coefficients will be derived for arbitrary incident fields.

The total wave field w is expressed in the form (3) where the incident and M source fields can be sought in terms of a complete expansion of separable solutions of the governing equation (2) in an appropriate coordinate system. Here it is convenient to use cylindrical coordinates and write

$$\tilde{w}(\mathbf{x}) = \sum_{n = -\infty}^{\infty} \left(A_n U_n^+(\mathbf{x}) + \mathcal{A}_n \mathcal{U}_n^+(\mathbf{x}) \right), \tag{4}$$

$$w_d(\mathbf{x}) = \sum_{m=1}^{M} \sum_{n=-\infty}^{\infty} \left(B_{m,n} V_n^+(\mathbf{x} - \mathbf{x}_m) + \mathcal{B}_{m,n} V_n^+(\mathbf{x} - \mathbf{x}_m) \right), \tag{5}$$

with

$$U_n^{\pm}(\mathbf{z}) = J_n(k|\mathbf{z}|) e^{\pm in \operatorname{arg} \mathbf{z}}, \quad U_n^{\pm}(\mathbf{z}) = I_n(k|\mathbf{z}|) e^{\pm in \operatorname{arg} \mathbf{z}},$$

$$V_n^{\pm}(\mathbf{z}) = H_n^{(1)}(k|\mathbf{z}|) e^{\pm in \operatorname{arg} \mathbf{z}}, \quad V_n^{\pm}(\mathbf{z}) = \frac{2i}{\pi} K_n(k|\mathbf{z}|) e^{\pm in \operatorname{arg} \mathbf{z}}$$
(6)

and where $H_n^{(1)}(|\mathbf{z}|) = J_n(|\mathbf{z}|) + \mathrm{i} Y_n(|\mathbf{z}|)$ is the Hankel function of the first kind and nth order, $I_n(|\mathbf{z}|) = \mathrm{i}^{-n} J_n(\mathrm{i}|\mathbf{z}|)$ and $2K_n(|\mathbf{z}|) = \pi \mathrm{i}^{n+1} H_n^{(1)}(\mathrm{i}|\mathbf{z}|)$. Note that this choice ensures that the incident field is indeed *incoming* from the far field whereas the active source fields are radiating away from their location. U_n and V_n are propagating modes whereas U_n and V_n are evanescent. The factor $2\mathrm{i}/\pi$ used in V_n^{\pm} merely ensures that subsequent algebra is cleaner. Here $\mathrm{arg}\,\mathbf{z}\in[0,2\pi)$ and $\mathrm{arg}(-\mathbf{z})=\mathrm{arg}\,\mathbf{z}\pm\pi\in[0,2\pi)$. Define

$$U_n^{\pm\prime}(\mathbf{z}) = J_n'(k|\mathbf{z}|)e^{\pm in \arg \mathbf{z}}, \quad U_n^{\pm\prime}(\mathbf{z}) = I_n'(k|\mathbf{z}|)e^{\pm in \arg \mathbf{z}}$$
(7)

and note the properties

$$U_n^{\pm}(-\mathbf{z}) = (-1)^n U_n^{\pm}(\mathbf{z}), \quad \mathcal{U}_n^{\pm}(-\mathbf{z}) = (-1)^n \mathcal{U}_n^{\pm}(\mathbf{z}),$$

$$V_n^{\pm}(-\mathbf{z}) = (-1)^n V_n^{\pm}(\mathbf{z}), \quad \mathcal{V}_n^{\pm}(-\mathbf{z}) = (-1)^n \mathcal{V}_n^{\pm}(\mathbf{z}).$$
(8)

In what follows Graf's addition theorems [26] are required, which are stated as

$$V_{\ell}^{+}(\mathbf{y} - \mathbf{x}) = \sum_{n = -\infty}^{\infty} \begin{cases} V_{n}^{+}(\mathbf{y})U_{n-\ell}^{-}(\mathbf{x}), & |\mathbf{y}| > |\mathbf{x}|, \\ U_{n}^{+}(\mathbf{y})V_{n-\ell}^{-}(\mathbf{x}), & |\mathbf{y}| < |\mathbf{x}|, \end{cases}$$
(9)

$$\mathcal{V}_{\ell}^{+}(\mathbf{y} - \mathbf{x}) = \sum_{n = -\infty}^{\infty} \begin{cases} \mathcal{V}_{n}^{+}(\mathbf{y})\mathcal{U}_{n-\ell}^{-}(\mathbf{x}), & |\mathbf{y}| > |\mathbf{x}|, \\ (-1)^{\ell}\mathcal{U}_{n}^{+}(\mathbf{y})\mathcal{V}_{n-\ell}^{-}(\mathbf{x}), & |\mathbf{y}| < |\mathbf{x}|. \end{cases}$$
(10)

The active source problem is now to determine the coefficients $B_{m,n}$ and $\mathcal{B}_{m,n}$ of (5) such that $w(\mathbf{x}) = 0$ for $\mathbf{x} \in \mathcal{C}$, where our calculations should also permit the determination of \mathcal{C} for a given distribution of source locations ($M \ge 3$).

3. Active cloaking

3.1. Integral equation formulation of the problem

All tensors arising in the following are defined with respect to the Cartesian basis introduced above. In order to determine the required source coefficients and the form of $\mathcal C$ the Rayleigh–Green theorem will be used so as to write down the form of the wave field in terms of an integral over the boundary of $\mathcal C$. As shall be shown shortly this form will be expressed in terms of various physical terms. In particular introduce the stress tensor $\sigma_{ij} = C_{ijkl} w_{,kl}(\mathbf x)$ where $C_{ijkl} = D(1-\nu)\delta_{ij}\delta_{kl} + \frac{1}{2}D\nu\left(\delta_{ik}\delta_{jl} + \delta_{il}\delta_{jk}\right)$ and $f_{,j}$ denotes the derivative of f with respect to x_j . The thickness averaged moment and shear components of the forces are then defined in terms of the stress as

$$m_{ij}(\mathbf{x}) = \int_{-h/2}^{h/2} \sigma_{ij}(\mathbf{x}, x_3) x_3 \, dx_3 = -D[(1 - \nu) w_{,ij} + \nu \delta_{ij} \nabla^2 w], \tag{11}$$

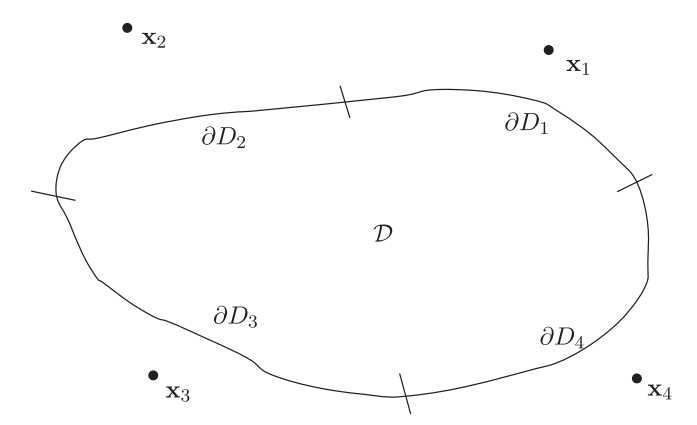


Fig. 3. A configuration of M=4 sources and a region \mathcal{D} in which the integral identity (15) holds.

$$q_i(\mathbf{x}) = \int_{-h/2}^{h/2} \sigma_{i3}(\mathbf{x}, x_3) \, \mathrm{d}x_3 = m_{ij,j}(\mathbf{x}) = -D\nabla^2 w_{,i}. \tag{12}$$

Summation over repeated indices is implied throughout unless otherwise stated.

Green's function associated with Eq. (2) satisfies the radiation condition and the governing partial differential equation

$$D(\nabla^2 \nabla^2 - k^4) G(\mathbf{x}, \mathbf{y}) = \delta(\mathbf{x} - \mathbf{y})$$
(13)

and is easily shown to be

$$G(\mathbf{x} - \mathbf{y}) = \gamma (V_0(\mathbf{x} - \mathbf{y}) + \mathcal{V}_0(\mathbf{x} - \mathbf{y})) \quad \text{with } \gamma = \frac{i}{8k^2 D}.$$
 (14)

With reference to Fig. 3 consider a region \mathcal{D} chosen so that it contains no sources. Explicit forms of the active source amplitudes will be determined together with the subset of \mathcal{D} that ensures cloaking. This region, already introduced as \mathcal{C} , is depicted in Fig. 2. By assumption w satisfies (2) in \mathcal{D} and therefore the Rayleigh–Green theorem [27] is invoked in order to write

$$w(\mathbf{x}) = \int_{\partial \mathcal{D}} [q(\mathbf{y})G(\mathbf{y} - \mathbf{x}) - Q(\mathbf{y})w(\mathbf{y})] dS + \int_{\partial \mathcal{D}} [w_{,i}(\mathbf{y})M_{ij}(\mathbf{y} - \mathbf{x}) - G_{,i}(\mathbf{y} - \mathbf{x})m_{ij}(\mathbf{y})] n_j dS.$$
(15)

Here $\partial \mathcal{D}$ is the boundary of \mathcal{D} as depicted in Fig. 3. It is the union of the arcs ∂D_m (note the difference between these and the arcs $\partial \mathcal{D}$ defined in Fig. 2). The vector \mathbf{n} is the normal exterior to $\partial \mathcal{D}$ and $q = q_i n_i$. Derivatives on the terms associated with Green's function are associated with \mathbf{y} . The moment and shear forces associated with Green's function have also been defined as

$$M_{ij}(\mathbf{y}-\mathbf{x}) = -D\left[(1-\nu)G_{,ij}(\mathbf{y}-\mathbf{x}) + \nu\partial_{ij}\nabla_{y}^{2}G(\mathbf{y}-\mathbf{x})\right], \qquad Q_{i}(\mathbf{y}-\mathbf{x}) = -D\nabla_{y}^{2}G_{,i}(\mathbf{y}-\mathbf{x})$$
(16)

where derivatives here are also defined with respect to **y**. Finally note that $Q = Q_i n_i$. Next introduce the following identities:

$$w_{i}M_{ii}n_{i} = \phi_{N}M_{N} + \phi_{T}M_{T}, G_{i}m_{ii}n_{i} = \Phi_{N}m_{N} + \Phi_{T}m_{T}$$

$$\tag{17}$$

where $m_N = m_{ij} n_i n_j$, $M_N = M_{ij} n_i n_j$ are the normal moments, $m_T = m_{ij} n_i t_j$, $M_T = M_{ij} n_i t_j$ are the twisting moments (t_j is the jth component of the tangent \mathbf{t} to $\partial \mathcal{D}$), $\phi_N = w_{,i} n_i$, $\Phi_N = G_{,i} n_i$ and $\phi_T = w_{,i} t_i$, $\Phi_T = G_{,i} t_i$. These allow the integral equation (15) to be simplified into the form

$$w(\mathbf{x}) = \int_{\partial D} [q(\mathbf{y})G(\mathbf{y} - \mathbf{x}) - Q(\mathbf{y} - \mathbf{x})w(\mathbf{y}) + \phi_T(\mathbf{y})M_T(\mathbf{y} - \mathbf{x}) - \Phi_T(\mathbf{y} - \mathbf{x})m_T(\mathbf{y}) + \phi_N(\mathbf{y})M_N(\mathbf{y} - \mathbf{x}) - \Phi_N(\mathbf{y} - \mathbf{x})m_N(\mathbf{y})] dS.$$
(18)

Physically this is a clean separation of three contributions to the field associated with shear forces, twisting moments and normal moments. Expression (18) can be employed for w, w_d and \tilde{w} since each satisfies the governing equation. The cloaked region C is that part of D in which the total field $w = \tilde{w} + w_d = 0$ so that

$$w_d(\mathbf{x}) = -\tilde{w}(\mathbf{x}) = -\int_{\partial \mathcal{C}} [\tilde{q}(\mathbf{y})G(\mathbf{y} - \mathbf{x}) - Q(\mathbf{y})\tilde{w}(\mathbf{y}) + \tilde{\phi}_T(\mathbf{y})M_T(\mathbf{y} - \mathbf{x}) - \Phi_T(\mathbf{y} - \mathbf{x})\tilde{m}_T(\mathbf{y}) + \tilde{\phi}_N(\mathbf{y})M_N(\mathbf{y} - \mathbf{x}) - \Phi_N(\mathbf{y} - \mathbf{x})\tilde{m}_N(\mathbf{y})] dS,$$

(19)

where on this occasion (18) has been employed for \tilde{w} . This therefore leads to the condition

$$w_{d}(\mathbf{x}) + \int_{\partial \mathcal{C}} \tilde{q}(\mathbf{y}) G(\mathbf{y} - \mathbf{x}) - Q(\mathbf{y} - \mathbf{x}) \tilde{w}(\mathbf{y}) \, dS + \int_{\partial \mathcal{C}} \tilde{\phi}_{T}(\mathbf{y}) M_{T}(\mathbf{y} - \mathbf{x}) - \Phi_{T}(\mathbf{y} - \mathbf{x}) \tilde{m}_{T}(\mathbf{y}) \, dS$$

$$+ \int_{\partial \mathcal{C}} \tilde{\phi}_{N}(\mathbf{y}) M_{N}(\mathbf{y} - \mathbf{x}) - \Phi_{N}(\mathbf{y} - \mathbf{x}) \tilde{m}_{N}(\mathbf{y}) \, dS = 0$$

$$(20)$$

which relates the active field w_d to the three contributions of the incident field associated with shear force, twisting moments and normal moments. As such (20) is conveniently written in the form

$$w_d(\mathbf{x}) + I_S(\mathbf{x}) + I_T(\mathbf{x}) + I_N(\mathbf{x}) = 0 \tag{21}$$

with the subscripts on I_S , I_T and I_N referring to shear, twist and normal respectively.

Recalling the form of w_d from (5) and motivated by the separation of the incident field into terms associated with shear force, twisting moments and normal moments write

$$B_{m,n} = B_{m,n}^{S} + B_{m,n}^{T} + B_{m,n}^{N}, \qquad B_{m,n} = B_{m,n}^{S} + B_{m,n}^{T} + B_{m,n}^{N}.$$
(22)

The aim is therefore to use (20) in order to choose each of the coefficients in (22) so that the associated contribution from the incident field is nullified in C.

3.2. General form of coefficients and requisite form of cloaked domain C

In order to evaluate the integrals in convenient form, use the first of each of (9) and (10) with $\ell = 0$ to rewrite Green's function, for $|\mathbf{y} - \mathbf{x}_m| < |\mathbf{x} - \mathbf{x}_m|$ as

$$G(\mathbf{y} - \mathbf{x}) = \gamma \sum_{n = -\infty}^{\infty} \left(U_n^{-}(\mathbf{y} - \mathbf{x}_m) V_n^{+}(\mathbf{x} - \mathbf{x}_m) + \mathcal{U}_n^{-}(\mathbf{y} - \mathbf{x}_m) \mathcal{V}_n^{+}(\mathbf{x} - \mathbf{x}_m) \right)$$
(23)

where γ is defined in (14). Combining (5) with (22) in (20) and using the form of Green's function (23) and incident field expansion (4) in the integrals of (20) it may straightforwardly be shown that the integrals can be written in the forms

$$\{I_{S}, I_{T}, I_{N}\}(\mathbf{x}) = -\sum_{m=1}^{M} \sum_{n=-\infty}^{\infty} \left(\{B_{m,n}^{S}, B_{m,n}^{T}, B_{m,n}^{N}\} V_{n}^{+}(\mathbf{x} - \mathbf{x}_{m}) + \{\mathcal{B}_{m,n}^{S}, \mathcal{B}_{m,n}^{T}, \mathcal{B}_{m,n}^{N}\} V_{n}^{+}(\mathbf{x} - \mathbf{x}_{m}) \right)$$

$$(24)$$

where the bracket notation indicates that for example

$$I_{S}(\mathbf{x}) = -\sum_{m=1}^{M} \sum_{n=-\infty}^{\infty} \left(B_{m,n}^{S} V_{n}^{+}(\mathbf{x} - \mathbf{x}_{m}) + \mathcal{B}_{m,n}^{S} \mathcal{V}_{n}^{+}(\mathbf{x} - \mathbf{x}_{m}) \right), \tag{25}$$

a notation that clearly permits great conciseness.

The coefficients associated with the shear term are

$$\{B_{m,n}^{S}, \mathcal{B}_{m,n}^{S}\} = \gamma \int_{\mathbb{R}^{d}} \left[\tilde{q}(\mathbf{y}) \{U_{n}^{-}, \mathcal{U}_{n}^{-}\} (\mathbf{y} - \mathbf{x}_{m}) + Dk^{2} \tilde{w}(\mathbf{y}) \mathbf{n} \cdot \nabla_{y} \{-U_{n}^{-}, \mathcal{U}_{n}^{-}\} (\mathbf{y} - \mathbf{x}_{m}) \right] dS_{y}$$

$$(26)$$

where it is noted that the integrals are now around the arcs ∂C_m as depicted in Fig. 2. These are oriented in the opposite manner to ∂C and hence a change in sign has been incorporated into the coefficients. This aspect also indicates the form of the cloaked region C as shall be described shortly. The change in sign in the last of (26) arises due to the use of $\nabla^2_y U_n^- = -k^2 U_n^-$ and $\nabla^2_y U_n^- = k^2 U_n^-$ therein.

Using $\mathbf{t} \cdot \mathbf{n} = 0$ in the twist term yields

$$\{B_{m,n}^T, \mathcal{B}_{m,n}^T\} = -\gamma \int_{\mathcal{X}} \left(D(1-\nu)\tilde{\boldsymbol{\phi}}_T(\mathbf{y}) \left[\mathbf{n} \cdot \nabla_y (\mathbf{t} \cdot \nabla_y \{U_n^-, \mathcal{U}_n^-\} (\mathbf{y} - \mathbf{x}_m)) \right] + \tilde{m}_T(\mathbf{y}) \left[\mathbf{t} \cdot \nabla_y \{U_n^-, \mathcal{U}_n^-\} (\mathbf{y} - \mathbf{x}_m) \right] \right) \, \mathrm{d}S_y. \tag{27}$$

Finally the normal moment contributions, using $\mathbf{n} \cdot \mathbf{n} = 1$, are

$$\{B_{m,n}^{N}, \mathcal{B}_{m,n}^{N}\} = -\gamma \int_{\partial \mathcal{C}_{m}} \tilde{m}_{N}(\mathbf{y}) \mathbf{n} \cdot \nabla_{y} \{U_{n}^{-}, \mathcal{U}_{n}^{-}\} (\mathbf{y} - \mathbf{x}_{m}) \, dS_{y} - \gamma \int_{\partial \mathcal{C}_{m}} \tilde{\phi}_{N}(\mathbf{y}) D(1 - \nu) \mathbf{n} \cdot \nabla_{y} (\mathbf{n} \cdot \nabla_{y} \{U_{n}^{-}, \mathcal{U}_{n}^{-}\} (\mathbf{y} - \mathbf{x}_{m})) \, dS_{y}
-\gamma \int_{\partial \mathcal{C}_{m}} \tilde{\phi}_{N}(\mathbf{y}) \nu Dk^{2} \{-U_{n}^{-}, \mathcal{U}_{n}^{-}\} (\mathbf{y} - \mathbf{x}_{m}) \, dS_{y}$$
(28)

where again the change in sign in the middle term on the right-hand side arises from the use of the governing equations. The integral form of the active scattering coefficients (26)–(28) must hold for all m and therefore the cloaked region $\mathcal C$ is exactly the subdomain of $\mathcal D$ in which Graf's theorem can be simultaneously invoked for all of the M active sources. As such $\mathcal C$ must be the region with boundary $\partial \mathcal C$ as the closed concave union of circular arcs defined by $\{a_m,\theta_m^{(1)},\theta_m^{(2)}\}$ which are denoted $\mathcal C_m$ and are depicted in Fig. 2.

In summary, the coefficients (26)–(28) determined here ensure that w=0 in the domain \mathcal{C} . However the fact that an explicit form for these coefficients has been derived in terms of integrals of the incident field over contours is of great utility. As will now be shown a general form for these coefficients can be derived and then more specific forms can be determined for given incident fields such as plane wave and point source incidence.

Introducing the notation

$$\alpha_m = ka_m, \tag{29}$$

the shear coefficients (26) become

$$\{B_{m,n}^{S}, \mathcal{B}_{m,n}^{S}\} = \gamma k D \alpha_{m} \{J_{n}(\alpha_{m}), I_{n}(\alpha_{m})\} \int_{\theta_{m}^{(1)}}^{\theta_{m}^{(2)}} \mathbf{n} \cdot \nabla_{y} \tilde{\mathbf{w}}(\mathbf{y}) e^{-in\theta} d\theta + \gamma k^{2} D \alpha_{m} \{-J'_{n}(\alpha_{m}), I'_{n}(\alpha_{m})\} \int_{\theta_{m}^{(1)}}^{\theta_{m}^{(2)}} \tilde{\mathbf{w}}(\mathbf{y}) e^{-in\theta} d\theta.$$
(30)

The twisting and normal moment coefficients (27) and (28) are

$$\{B_{m,n}^{T}, \mathcal{B}_{m,n}^{T}\} = \operatorname{in}\gamma \left(\{J_{n}(\alpha_{m}), I_{n}(\alpha_{m})\} \int_{\theta_{m}^{(1)}}^{\theta_{m}^{(2)}} \tilde{m}_{T}(\mathbf{y}) e^{-\operatorname{i}n\theta} d\theta + D(1-\nu)k \left\{ J_{n}'(\alpha_{m}) - \frac{J_{n}(\alpha_{m})}{\alpha_{m}}, I_{n}'(\alpha_{m}) - \frac{I_{n}(\alpha_{m})}{\alpha_{m}} \right\} \int_{\theta_{m}^{(1)}}^{\theta_{m}^{(2)}} \tilde{\phi}_{T}(\mathbf{y}) e^{-\operatorname{i}n\theta} d\theta \right)$$

$$(31)$$

and

$$\{B_{m,n}^{N}, \mathcal{B}_{m,n}^{N}\} = -\gamma \alpha_{m} \left\{ \{J'_{n}(\alpha_{m}), I'_{n}(\alpha_{m})\} \int_{\theta_{m}^{(1)}}^{\theta_{m}^{(2)}} \tilde{m}_{N}(\mathbf{y}) e^{-in\theta} d\theta + Dk \left[(1-\nu)\{J'_{n}(\alpha_{m}), I'_{n}(\alpha_{m})\} + \nu \{-J_{n}(\alpha_{m}), I_{n}(\alpha_{m})\} \right] \int_{\theta_{m}^{(1)}}^{\theta_{m}^{(2)}} \tilde{\phi}_{N}(\mathbf{y}) e^{-in\theta} d\theta \right\}.$$
(32)

Finally a check has to be made that the active source field vanishes in some region away from the cloaked region. Note that the Rayleigh–Green theorem holds for all \mathbf{x} . However Graf's addition theorem has been used and therefore, rigorously speaking, the specified expressions are available only for \mathbf{x} in the region $\mathbb{R}^2/\cup_{i=1}$... ${}_n\mathcal{D}_i$ with $\mathcal{D}_i=\{\mathbf{x}\in\mathbb{R}^2,|\mathbf{x}-\mathbf{x}_i|\}$. This latter region is therefore $\mathcal{C}\cup\mathcal{R}$ as defined in Fig. 2. As was first observed for $\mathbf{x}\in\mathcal{C}$, the active field therefore cancels the incoming wave due to the Rayleigh–Green theorem (15). On the other hand if $\mathbf{x}\in\mathcal{R}$ then \mathbf{x} is not in the domain bounded by $\partial\mathcal{C}$ corresponding to the integration domain and the Rayleigh–Green theorem ensures that the integral (15) is zero. Therefore the active source field is zero in the far-field region \mathcal{R} . It is not possible to comment on the field close to the source regions because Graf's addition theorem has been used here. One can say only that as the number of multipole sources increases the field diverges inside these source regions, see Section 3.5 for brief further discussion on this point.

To conclude, given a specific incident field \tilde{w} , an active cloak is constructed by first choosing the number $M \ge 3$ of active sources and their locations. The active field then takes the form (5) where the source amplitudes are given by (22) and where for convenience the contributions are separated into contributions given by (30)–(32) which can be evaluated straightforwardly. This is now done for two specific cases of interest, plane wave incidence and point source incidence.

3.3. Plane wave incidence

Consider an incident plane-wave of unit amplitude in the direction ψ ,

$$\tilde{w}(\mathbf{x}) = w_{w}(\mathbf{x}) = e^{\mathrm{i}k\hat{\mathbf{e}}(\psi)\cdot\mathbf{x}} \tag{33}$$

where it is recalled that $\hat{\mathbf{e}}(\psi) = (\cos \psi, \sin \psi)$ is a unit direction vector. This means that it is possible to write $\tilde{w}(\mathbf{y}) = \tilde{w}(\mathbf{x}_m)\tilde{w}(\mathbf{a}_m)$ for $\mathbf{y} \in \partial \mathcal{C}_m$, where $\mathbf{a}_m = a_m \hat{\mathbf{e}}(\theta)$. For ease of reading the details of the calculations are not developed here; the reader is referred to the Appendix. It transpires that the source coefficients are

$$\{B_{m,n}^{S}, \mathcal{B}_{m,n}^{S}\} = \frac{i}{8} \alpha_{m} w_{\psi}(\mathbf{x}_{m}) \Big[\{J_{n}(\alpha_{m}), I_{n}(\alpha_{m})\} L_{mn}^{01}(\alpha_{m}) + \{-J'_{n}(\alpha_{m}), I'_{n}(\alpha_{m})\} L_{mn}^{00}(\alpha_{m}) \Big], \tag{34}$$

$$\{B_{m,n}^{T}, \mathcal{B}_{m,n}^{T}\} = -\frac{\mathrm{i}}{8}(1-\nu)nw_{\psi}(\mathbf{x}_{m})\left[\{J_{n}(\alpha_{m}), I_{n}(\alpha_{m})\}L_{mn}^{11}(\alpha_{m}) + \left\{\frac{J_{n}(\alpha_{m})}{\alpha_{m}} - J_{n}'(\alpha_{m}), \frac{I_{n}(\alpha_{m})}{\alpha_{m}} - I_{n}'(\alpha_{m})\right\}L_{mn}^{10}(\alpha_{m})\right], \tag{35}$$

$$\{B_{m,n}^{N},\mathcal{B}_{m,n}^{N}\} = \{\nu B_{m,n}^{S}, -\nu \mathcal{B}_{m,n}^{S}\} - \frac{\mathrm{i}}{8}(1-\nu)\alpha_{m}w_{\psi}(\mathbf{x}_{m}) \left[\{J_{n}^{'}(\alpha_{m}), I_{n}^{'}(\alpha_{m})\}L_{mn}^{01}(\alpha_{m}) + \{J_{n}^{'}(\alpha_{m}), I_{n}^{'}(\alpha_{m})\}L_{mn}^{02}(\alpha_{m}) \right]$$
(36)

where

$$L_{mn}^{ij}(\alpha_m) = i^j \int_{\theta_m^{(1)} - \mu \nu}^{\theta_m^{(2)} - \psi} \sin^i \theta \cos^j \theta e^{i[\alpha_m \cos \theta - n(\theta + \psi)]} d\theta.$$
 (37)

Explicit expressions for these integrals are given in the Appendix.

3.4. Point source incident field

Consider now that a point source, located at $\mathbf{x} = \mathbf{x}_s \in \mathcal{R}$ generates the incident wave and suppose that it is sufficiently far away from the domain of scatterers that any contribution to the incident field from the evanescent terms is negligible. That is, take $A_n = 0$ for all n. The incident field can therefore be represented in the general form

$$\tilde{w}(\mathbf{y}) = \sum_{\ell=-\infty}^{\infty} A_{\ell} V_{\ell}^{+}(\mathbf{y} - \mathbf{x}_{s}). \tag{38}$$

Furthermore since $\mathbf{x}_s \in \mathcal{R}$, for every $m \in \{1, 2, ..., M\}$ it is clear that $a_m < |\mathbf{x}_s - \mathbf{x}_m|$. Therefore Graf's theorem is applied to deduce that for $\mathbf{y} = \mathbf{x}_m + \mathbf{a}_m \in \partial \mathcal{C}_m$

$$\tilde{w}(\mathbf{y}) = \sum_{n = -\infty}^{\infty} \tilde{A}_n U_n^+(\mathbf{a}_m) \quad \text{with } \tilde{A}_n = \sum_{\ell = -\infty}^{\infty} A_{\ell} (-1)^{n-\ell} V_{n-\ell}^-(\mathbf{x}_m - \mathbf{x}_s). \tag{39}$$

As in the theory developed in [15] the general active field for the point source incident wave may be derived simply by exploiting linearity, integrating the source coefficients for plane wave incidence (34)–(36) with respect to ψ and using the expression

$$\frac{i^{-n}}{2\pi} \int_0^{2\pi} d\psi \ w_{\psi}(\mathbf{x}) e^{im\psi} = U_n^+(\mathbf{x}). \tag{40}$$

This gives

$$w_d(\mathbf{x}) = \sum_{m=1}^{M} \sum_{n,p=-\infty}^{\infty} (B_{m,np}^S + B_{m,np}^T + B_{m,np}^N) V_n^+(\mathbf{x} - \mathbf{x}_m)$$
(41)

where

$$\{B_{m,np}^S, B_{m,np}^T, B_{m,np}^N\} = \tilde{A}_p \frac{i^{-p}}{2\pi} \int_0^{2\pi} \{B_{m,n}^S, B_{m,n}^T, B_{m,n}^N\} e^{ip\psi} d\psi. \tag{42}$$

3.5. Divergence of the active field summation

As was noted in Section 3.6 of [16], the infinite sum expression for the active source fields defined by (5) with source amplitudes (26)–(28) is formally valid only in $|\mathbf{x}-\mathbf{x}_m| > a_m$. That is, the expression is not itself valid in the domains \mathcal{D}_m in which the sources reside! A valid form could be obtained by using the alternative version of Graf's addition theorem in the domain \mathcal{D}_m associated with the arc $\partial \mathcal{C}_m$ but with use of the usual form of Graf in the domain \mathcal{A}_m , associated with all other $\partial \mathcal{C}_n$, $n \neq m$. We would then be assured that the active field is zero everywhere outside \mathcal{C} . However if this was done, the mth source would not be present in the domain \mathcal{D}_m since the active field would be bounded by construction.

Active cloaking for flexural waves via the method proposed above therefore requires that the expression (5) with source amplitudes given by Eqs. (22), (34)–(36) is employed for the active field everywhere but a finite number of terms must be taken in the multipole expansion in order to ensure that it does not diverge. The source amplitudes that appear in the infinite sum are used as motivation for the choice of source amplitudes that should be chosen in an active field that contains only a finite number of multipoles. This ensures a finite (but large) field inside the source regions. As noted before this issue was discussed in [21]. With a finite multipole sum for the active field therefore, perfect cloaking is not achieved *but*

$$w(\mathbf{x}) \approx \begin{cases} 0, & \mathbf{x} \in \mathcal{C}, \\ \mathbf{w}_i(\mathbf{x}), & \mathbf{x} \in \mathcal{R}. \end{cases}$$
 (43)

The field is large (but finite) inside the domain $\bigcup_{i=1..n} \mathcal{D}_i$. Finally note that a straightforward truncation of the active field may not be optimal in terms of cloaking and ensuring a non-radiating field.

4. Necessary and sufficient conditions on source amplitudes for active cloaking

Without loss of generality suppose that the origin of the coordinate system is located inside the cloaked region C and therefore $a_m < |\mathbf{x}_m|$. As such the following theorems can then be stated regarding conditions on the source amplitudes.

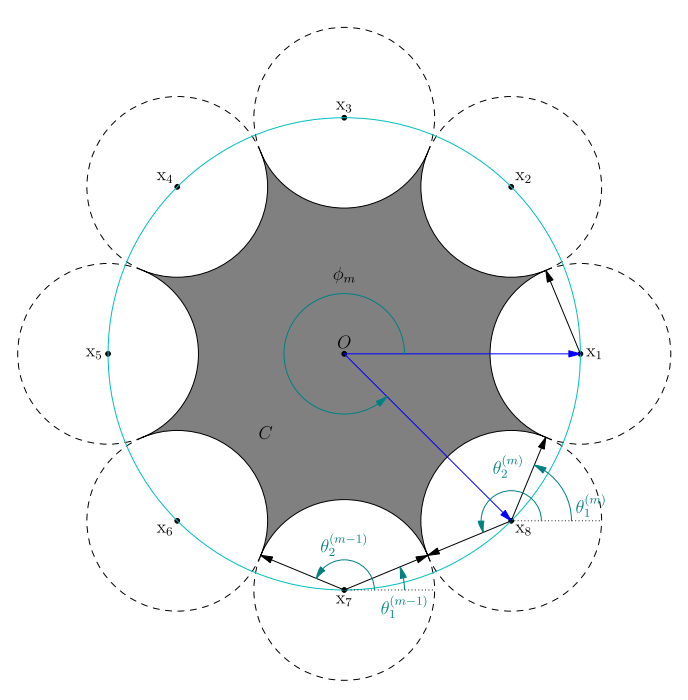


Fig. 4. Typical configuration used for numerical implementation of the scheme, in this case for eight active sources.

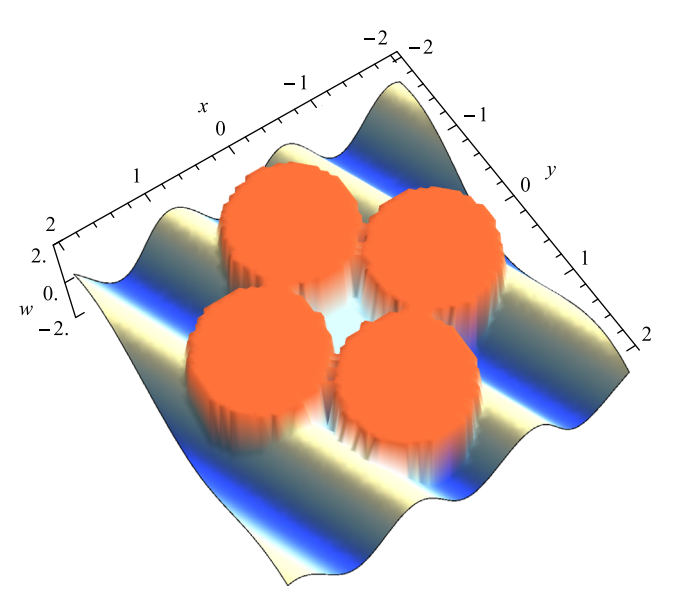


Fig. 5. The total field with 4 active sources, angle of incidence $\psi = \pi/8$, wavenumber kr = 5 and N = 50. Since values in the source regions can become extremely large compared with the incident field, the source regions are simply shown in red here. (For interpretation of the references to colour in this figure caption, the reader is referred to the web version of this paper.)

Theorem 1. Sufficient conditions for the active cloak to be non-radiating are

$$\forall n \in \mathbb{Z}: \quad \sum_{m=1}^{M} \sum_{\ell=-\infty}^{\infty} \begin{cases} B_{m,\ell} \ U_{n-\ell}^{-}(\mathbf{x}_{m}) = 0, \\ B_{m,\ell} \ U_{n-\ell}^{-}(\mathbf{x}_{m}) = 0 \end{cases}$$

$$(44)$$

whilst only the first of these is necessary, as shall now be proved.

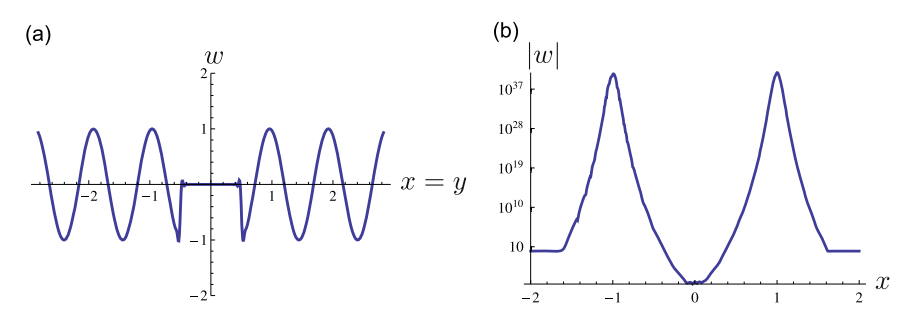


Fig. 6. With kr = 5 and N = 50, plots of (a) the absolute value of the total field |w| along x = y and (b) the total field w at y = 0.1 with a log scale for clarity.

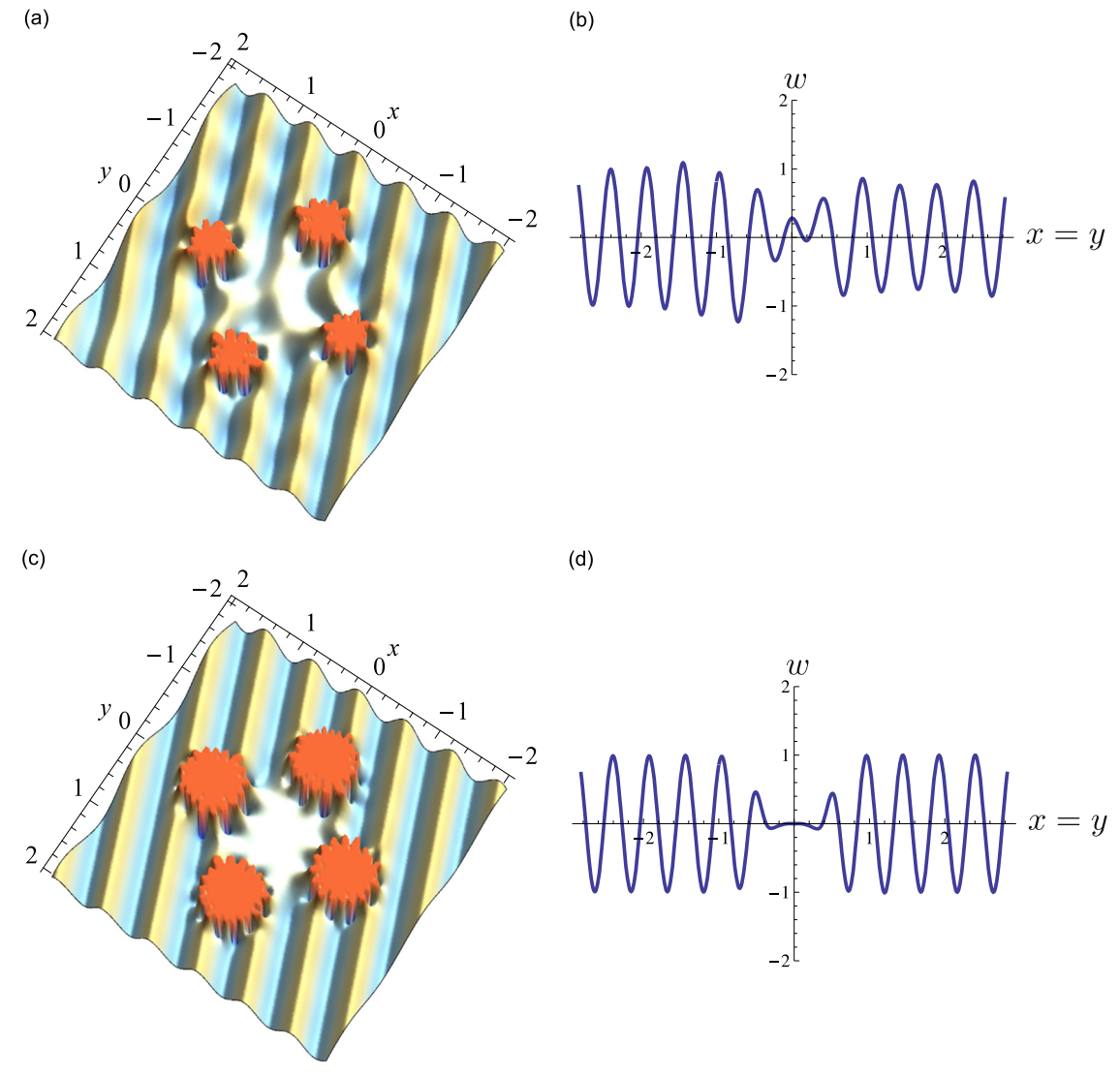


Fig. 7. With kr = 10 and M = 4, (a) surface plot of w with N = 5, (b) plot of w along the line x = y with N = 5, (c) surface plot of w with N = 10 and (d) plot of w along the line x = y with N = 10. One can see that the effect of doubling the number of multipoles is to ensure a much greater cloaking effect as well as ensuring that the field exterior is the pure incident field.

A similar procedure is followed to that in [15]. The first of Graf's addition theorems (9) and (10) enables the active field $w_d(\mathbf{x})$ to be written in an appropriate form in the far field, i.e.

$$w_d(\mathbf{x}) = \sum_{n=-\infty}^{\infty} \left(F_n V_n^+(\mathbf{x}) + \mathcal{F}_n V_n^+(\mathbf{x}) \right). \tag{45}$$

This expression applies for $|\mathbf{x}| > \max(|\mathbf{x}_m + \mathbf{a}_m|)$ where

$$F_{n} = \sum_{m=1}^{M} \sum_{\ell=-\infty}^{\infty} B_{m,\ell} U_{n-\ell}^{-}(\mathbf{x}_{m}), \qquad \mathcal{F}_{n} = \sum_{m=1}^{M} \sum_{\ell=-\infty}^{\infty} \mathcal{B}_{m,\ell}, \mathcal{U}_{n-\ell}^{-}(\mathbf{x}_{m}). \tag{46}$$

The sufficiency of (44) follows immediately by substituting these forms into the right-hand sides of (46), giving zero radiated field from the active sources, $F_n = 0$ and $\mathcal{F}_n = 0$.

As regards necessity, first assume that w_d does not radiate energy into the far field in \mathcal{R} . Writing $\theta = \arg \mathbf{x}$, the far-field form of $w_d(\mathbf{x})$ is

$$w_d(\mathbf{x}) = f(\theta) \frac{e^{ik|\mathbf{x}|}}{(k|\mathbf{x}|)^{1/2}} + g(\theta) \frac{e^{-k|\mathbf{x}|}}{(k|\mathbf{x}|)^{1/2}} + O((k|\mathbf{x}|)^{-3/2})$$
(47)

where

$$\{f(\theta), g(\theta)\} = \sum_{n = -\infty}^{\infty} \{f_n, g_n\} e^{in\theta}, \qquad \{f_n, g_n\} = \left(\frac{2}{\pi}\right)^{1/2} \{i^{-(n+1/2)}F_n, i\mathcal{F}_n\}. \tag{48}$$

The power radiated into the far field only involves $f(\theta)$ and $not\ g(\theta)$ and therefore although $F_n = 0$ is required for all n (which therefore dictates the necessity of the first of (44)), $\mathcal{F}_n = 0$ is not a necessary condition due to the exponential decay of the evanescent terms.

Theorem 2. Necessary and sufficient conditions on the source coefficients to ensure that the incident wave is cancelled in the near-field (cloak) domain C are

$$\forall n \in \mathbb{Z}: \quad \sum_{m=1}^{M} \sum_{\ell=-\infty}^{\infty} \begin{cases} B_{m,\ell} \ V_{n-\ell}^{-}(\mathbf{x}_{m}) = -A_{n}, \\ (-1)^{\ell} \mathcal{B}_{m,\ell} \ V_{n-\ell}^{-}(\mathbf{x}_{m}) = -\mathcal{A}_{n}. \end{cases}$$
(49)

Assume that the source coefficients satisfy (49). With $\mathbf{x} \in \mathcal{C}$, the near field, then $|\mathbf{x}| < \min(|\mathbf{x}_m - \mathbf{a}_m|)$ and the second of Graf's addition theorems (9) and (10) are used to write the near-field form as

$$w_d(\mathbf{x}) = \sum_{n = -\infty}^{\infty} \left(E_n U_n^+(\mathbf{x}) + \mathcal{E}_n \mathcal{U}_n^+(\mathbf{x}) \right), \tag{50}$$

where

$$E_{n} = \sum_{m=1}^{M} \sum_{l=-\infty}^{\infty} B_{m,l} V_{n-l}^{-}(\mathbf{x}_{m}), \qquad \mathcal{E}_{n} = \sum_{m=1}^{M} \sum_{l=-\infty}^{\infty} (-1)^{\ell} \mathcal{B}_{m,l} V_{n-l}^{-}(\mathbf{x}_{m}).$$
 (51)

Next use the forms (49) which therefore gives $A_n + E_n = 0$ and $A_n + E_n = 0$, the total field is nullified in the cloaked region. As for necessity, assume that $\tilde{w} + w_d = 0$ in C. With $\mathbf{x} \in C$ the form for the active field is as in (50). Combining this with the general form for the incident field stated in (4) and setting $\tilde{w} + w_d = 0$ means that (49) is required to hold due to the linear independence of $U_n(\mathbf{x})$ and $U_n(\mathbf{x})$.

5. Implementation and specific examples

5.1. Active source configuration

We illustrate the result for plane wave incidence on configurations of the type shown in Fig. 4. The M sources are symmetrically located on a circle. Thus for $m \in \{1,...M\}$

$$a_m = a$$
, $|\mathbf{x}_m| = r$, $\phi_m = (m-1)\phi_0$ with $\phi_0 = \frac{2\pi}{M}$,

and by necessity $a = r \sin{(\pi/M)}$. By symmetry the circular arcs all have the same angular extent whose angles are defined by

$$\theta_{1,2}^{(m)} = \pi + \phi_m \mp \left| \frac{\pi}{2} - \frac{\pi}{M} \right|. \tag{52}$$

Note that the cloaked region C can be formed by a minimum of three sources. A configuration with M=8 is shown in Fig. 4.

5.2. Analysis of the total field

Consider unit amplitude plane-wave incidence from an angle $\psi = \pi/8$ and without loss of generality take r=1 with configurations of active sources of the type described in Section 5.1. Several examples will be considered in order to illustrate the extent of the cloaking effect.

Most fundamentally the true active source field (5) cannot be employed in practice because there will be a limitation on the number of modes that can be employed. Indeed, traditional anti-vibration techniques struggle to go beyond dipoles, for example. As such define the field

$$W_d^{\text{app}}(\mathbf{x}) = \sum_{m=1}^{M} \sum_{n=-N}^{N} (B_{m,n} V_n^+(\mathbf{x} - \mathbf{x}_m) + \mathcal{B}_{m,n} V_n^+(\mathbf{x} - \mathbf{x}_m)),$$
 (53)

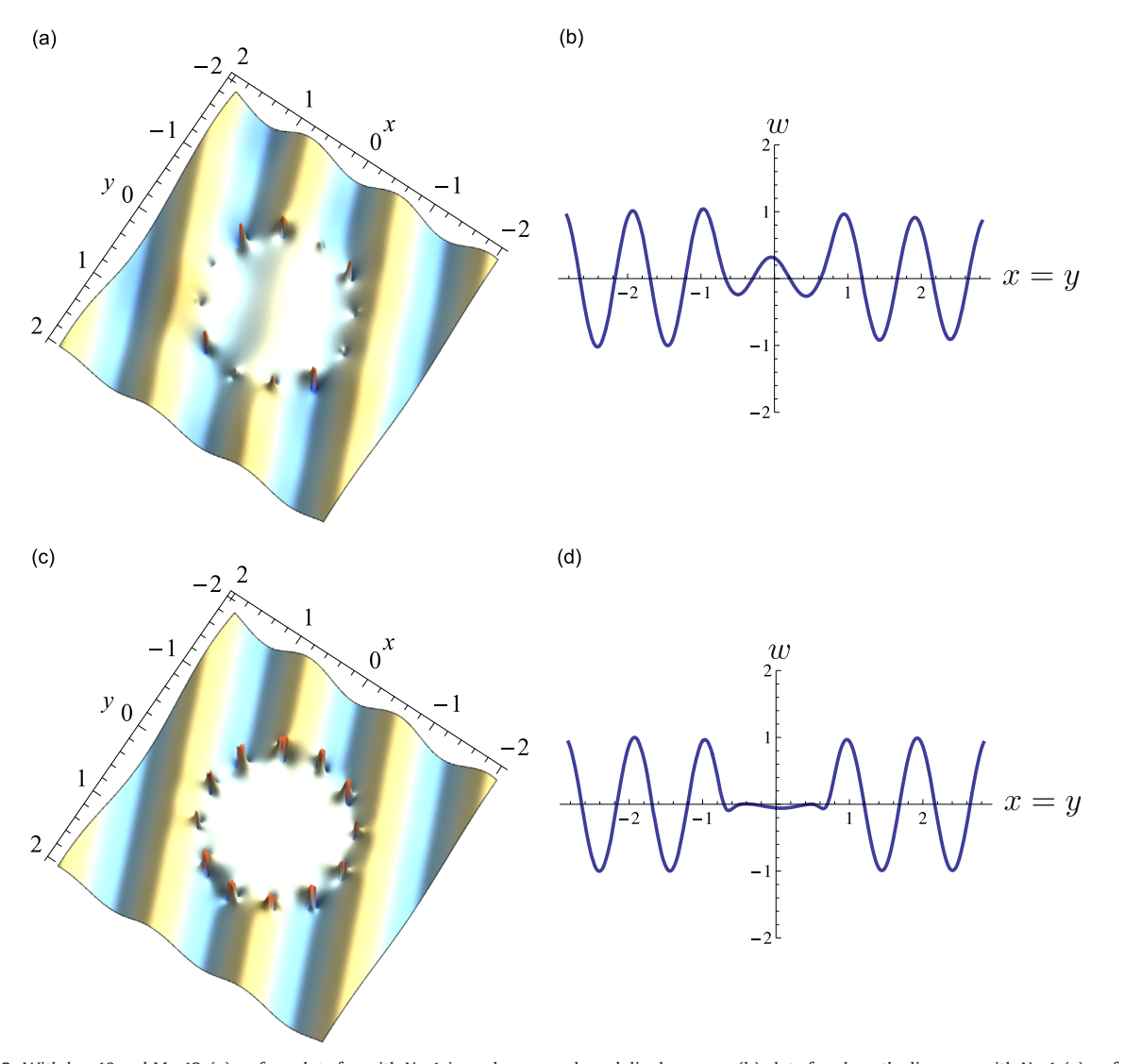


Fig. 8. With kr=10 and M=12, (a) surface plot of w with N=1, i.e. only monopole and dipole sources (b) plot of w along the line x=y with N=1, (c) surface plot of w with N=2 and (d) plot of w along the line x=y with N=2. One can see that having a large number of sources means that far less multipoles are required. The additional $n=\pm 2$ mode appears to have a significant effect in terms of ensuring that the total field is close to zero in C.

and subsequent investigations now centre on how effective such active cloaking is, for combinations of M and N given a value of the parameter kr.

First consider the case when four active sources are employed with kr=5 and N=50, i.e. a large expansion of multipoles, for which it is expected that the cloaking effect should be excellent. A surface plot of the (real part of the) total field is plotted in Fig. 5 where it is clearly seen that the incident wave is undisturbed outside the exterior region \mathcal{R} . In the source regions the field is somewhat erratic and often large, as a result of the formal divergence of the field in this region as N becomes large as discussed in Section 3.5 and therefore a constant value of |w|=2 has been plotted in those regions for clarity in order to emphasize the field outside these domains; source regions will be discussed again shortly. From the figure it is clearly seen that the total field is nullified in the cloaked region \mathcal{C} , the region bounded by the inner arcs of the source domains. Fig. 6 illustrates this behaviour further. In (a) the total field is plotted along the line x=y and indicates that the total field is zero in the inner region \mathcal{C} . A sudden transition to the incident field outside \mathcal{C} , i.e. in \mathcal{R} is clearly visible. In (b) the absolute value of the field is plotted along the line y=0.1, using a log scale for |w| in order to illustrate the size of the field inside the source regions. It should be noted that $|w|=|\tilde{w}|=1$ in the region exterior to the source regions and $|w|\approx 0$ in the inner cloaked region, an approximation that would be further improved for a larger value of N.

The ability to generate multipole sources up to N=50 in reality is clearly questionable and therefore in Fig. 7 lower values of truncation are used, N=5 and N=10 in the case when kr=10, i.e. at higher frequency. The footprint of the source region is clearly seen to be reduced significantly as compared with the N=50 case. Reducing the number of modes clearly gives a less beneficial cloaking effect. If N is to be reduced further then for the cloaking effect to remain significant it is clear that a larger number of active sources must be employed. This effect is studied in Fig. 8 where twelve sources are used in the case when

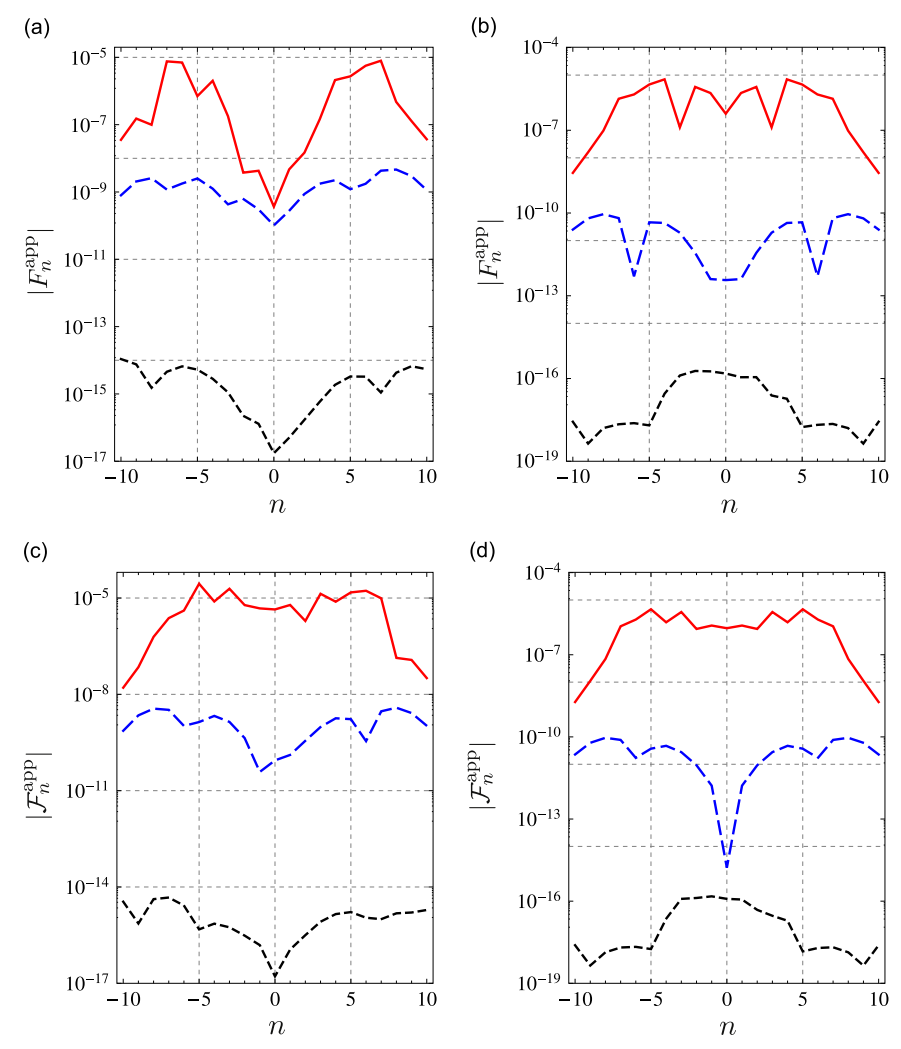


Fig. 9. Absolute values of the far-field coefficients, $|F_n^{app}|$ (top) and $|\mathcal{F}_n^{app}|$ (bottom) with kr = 1, red/solid: N = 5, blue/dashed: N = 10, black/dotted: N = 15. (a) M = 3, (b) M = 6, (c) M = 3 and (d) M = 6. (For interpretation of the references to colour in this figure caption, the reader is referred to the web version of this paper.)

kr=5. In (a) and (b) the simple case of N=1 is taken whereas in (c) and (d) N=2. It is notable that the cloaking effect is rather good in the case N=2, so that the number of sources compensates for the lack of modes, as should be expected.

5.3. Near- and far-field modal amplitudes

It has been shown schematically that the cloaking effect can be achieved in a fairly simple manner by either choosing a small number of sources with N large or a large number of sources with N small, the latter perhaps being the most practical to perform. It is clearly seen that the active sources are non-radiating and the total field in the cloaked domain \mathcal{C} is negligible for appropriate combinations of M and N. Here the efficiency of the cloaking mechanism is considered by focusing on what are termed the far-field (F_n, \mathcal{F}_n) and near-field (E_n, \mathcal{E}_n) coefficients defined in (46) and (51) respectively.

If all terms in the active field (5) and therefore in the infinite sums in equations (44) are included then the far field is exactly zero and the incident wave is fully cancelled by the active sources. In practice, as in (53) these sums must be truncated at order N, limiting the order of multipole sources, so that the associated far-fields and near-fields associated with the active sources w_d are approximated by

$$\forall n \in \mathbb{Z}: \quad \sum_{m=1}^{M} \sum_{l=-N}^{N} \begin{cases} B_{m,l} V_{n-l}^{-}(\mathbf{x}_{m}) = E_{n}^{\text{app}}, \\ \mathcal{B}_{m,l} V_{n-l}^{-}(\mathbf{x}_{m}) = \mathcal{E}_{n}^{\text{app}}, \\ B_{m,l} U_{n-l}^{-}(\mathbf{x}_{m}) = F_{n}^{\text{app}}, \\ \mathcal{B}_{m,l} U_{n-l}^{-}(\mathbf{x}_{m}) = \mathcal{F}_{n}^{\text{app}}. \end{cases}$$
(54)

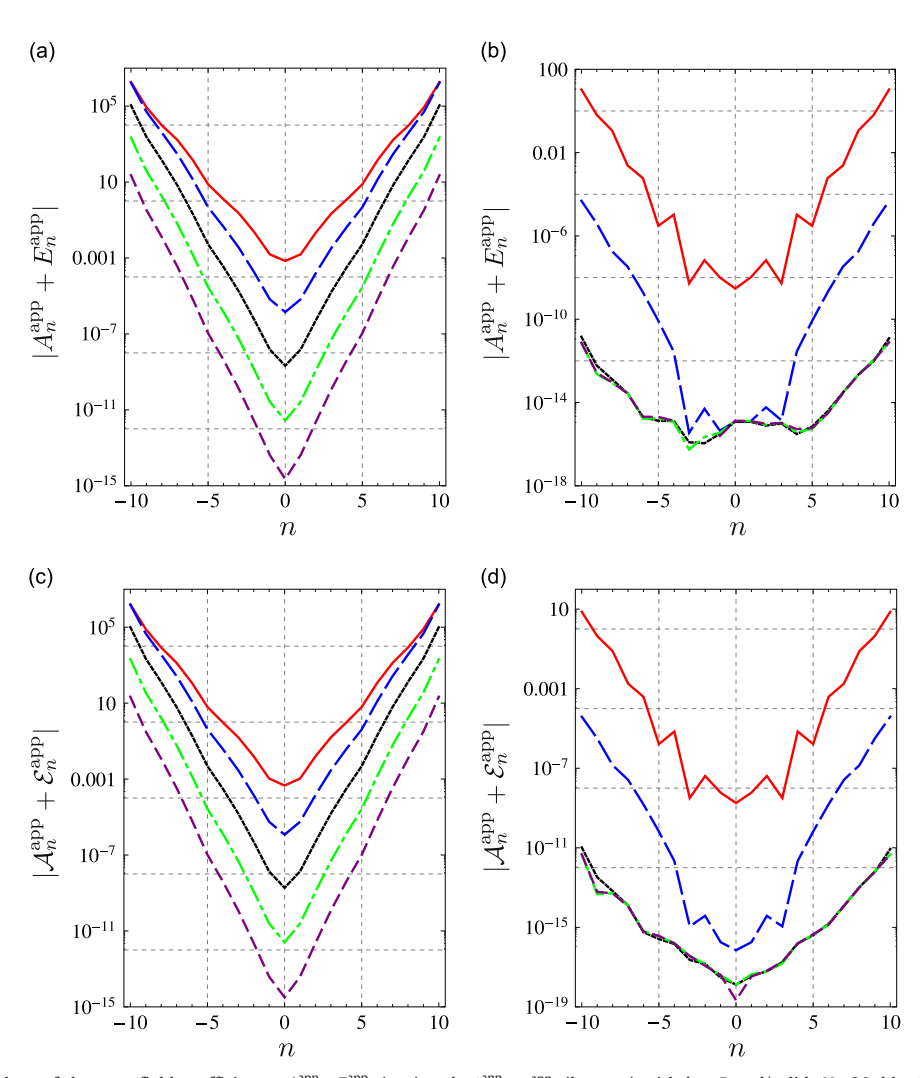


Fig. 10. Absolute values of the near-field coefficients, $|A_n^{app} + E_n^{app}|$ (top) and $|A_n^{app} + E_n^{app}|$ (bottom) with kr = 5, red/solid: N = 20, blue/long dashed: N = 40, black/solid: N = 60, green/dot-dashed: N = 80, magenta/short dashed: N = 100. (a) M = 4, (b) M = 8, (c) M = 4 and (d) M = 8. (For interpretation of the references to colour in this figure caption, the reader is referred to the web version of this paper.)

Given the incoming frequency kr and with ka and M arranged as in Fig. 4 (other configurations are possible of course) then the cloaking strategy relies upon the subsequent choice of M, N. As such, in order to assess the efficiency of the cloaking the far- and near-fields are examined as functions of these parameters.

As has been proven in the theorems in Section 4, it is necessary and sufficient that for each n,

$$\{F_n^{\text{app}}, \mathcal{F}_n^{\text{app}}, E_n^{\text{app}} + A_n, \mathcal{E}_n^{\text{app}} + A_n\} \to 0 \text{ as } N \to \infty,$$
 (55)

noting that for plane-wave incidence,

$$A_n = i^n e^{-in\psi}, \quad A_n = 0. \tag{56}$$

Consider first the far-field conditions. In Fig. 9 the coefficients $|\mathcal{F}_n^{app}|$ and $|\mathcal{F}_n^{app}|$ are plotted for each $n \in \{-10, ..., 10\}$ for M=3 (left) and M=6 (right) with kr=1 and each curve is associated with a different truncation N. As should be expected, as both M and N are increased the effect of cloaking is improved. It is notable that when N is relatively small (e.g. N=5) even a modest number of sources achieves weak far-field scattering associated with the active field (considering that the incident field is of unit amplitude). The convergence of the far-field coefficients to zero as N increases is rapid as can be seen and furthermore the effect is fairly uniform for any value of n.

Turning now to the near-field cloaking effect, a number of results are illustrated in Figs. 10–12. Each curve in Fig. 10 is associated with a different truncation value N, highlighting the effect of varying N on the coefficients $|A_n^{\rm app} + E_n^{\rm app}|$ and $|A_n^{\rm app} + E_n^{\rm app}|$ at a fixed value of kr=5 for M=4 (left) and M=8 (right). The comparative effect of varying the number of sources M is shown in Fig. 11 for a fixed value N=100 with kr=5 (left) and kr=10 (right). Finally, Fig. 12 compares the near-field coefficients as a function of kr with fixed N=100 and for M=3 (left) and M=6 (right).

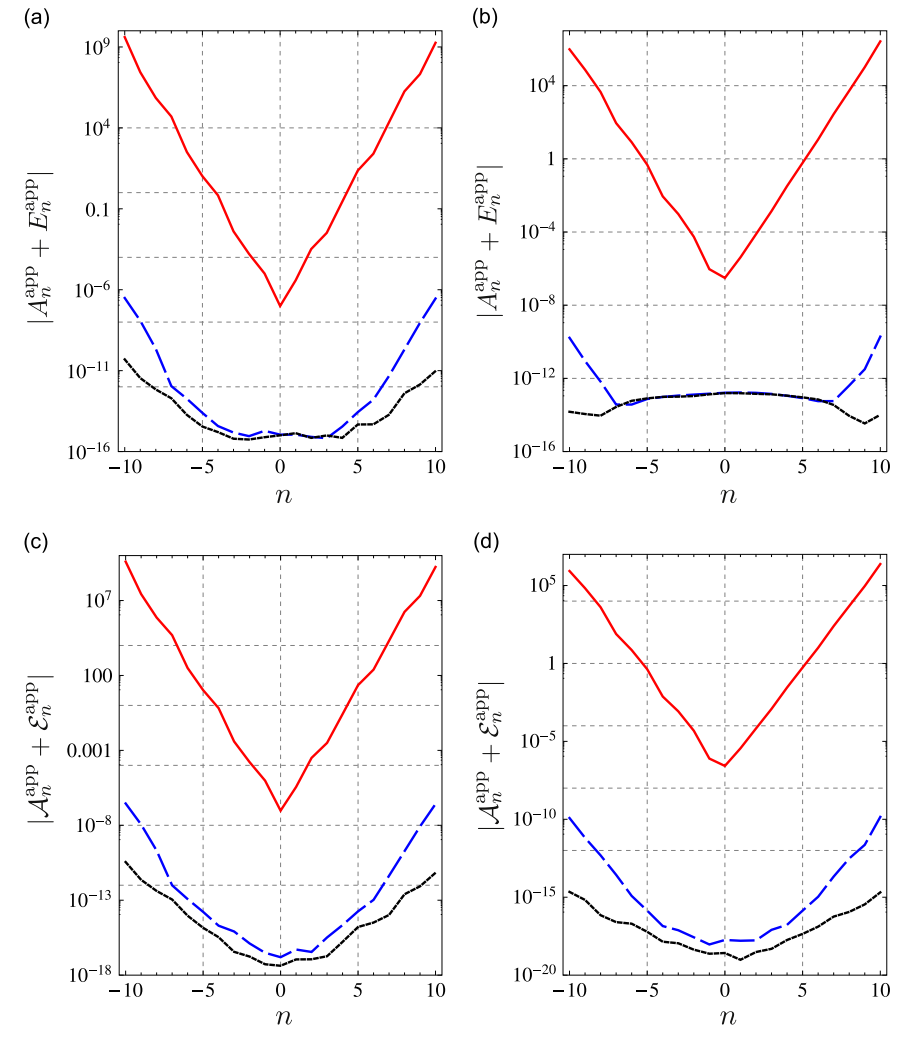


Fig. 11. Absolute values of the near-field coefficients, $|A_n^{app} + \mathcal{E}_n^{app}|$ (top) and $|A_n^{app} + \mathcal{E}_n^{app}|$ (bottom), with N = 100 and kr = 5 (left) and kr = 10 (right), red/solid: M = 3, blue/long dashed: M = 5, black/solid: M = 7. (a) kr = 5, (b) kr = 10, (c) kr = 5 and (d) kr = 10. (For interpretation of the references to colour in this figure caption, the reader is referred to the web version of this paper.)

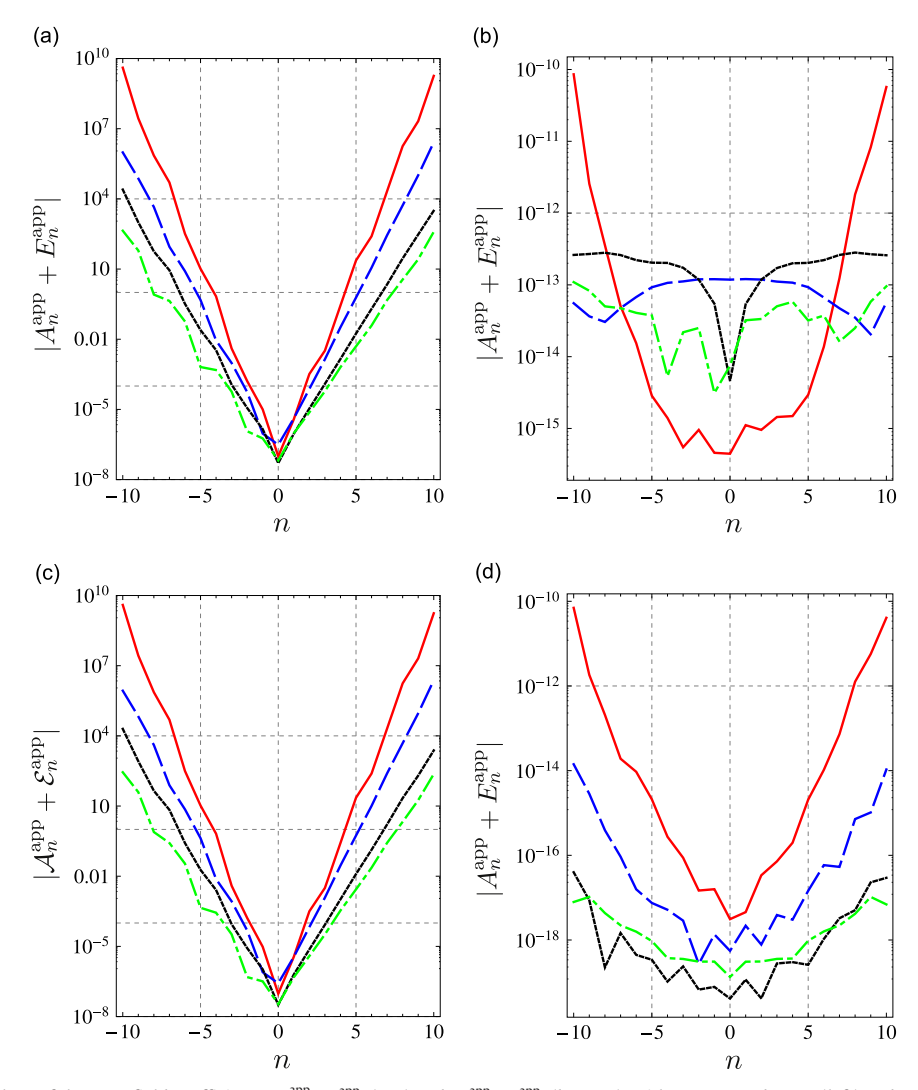


Fig. 12. Absolute values of the near-field coefficients, $|A_n^{\text{app}} + E_n^{\text{app}}|$ (top) and $|A_n^{\text{app}} + E_n^{\text{app}}|$ (bottom), with N = 100 and M = 3 (left) and M = 6 (right), red/solid: kr = 5, blue/long dashed: kr = 10, black/solid: kr = 15, green/dot-dashed: kr = 20. (a) M = 3, (b) M = 6, (c) M = 3 and (d) M = 6. (For interpretation of the references to colour in this figure caption, the reader is referred to the web version of this paper.)

Several features are evident from the near-field plots in Figs. 10–12. First, notice in each case that the near-field coefficients increase in magnitude with $|n| \le N$ which is not the case for the far-field coefficients. In particular, the magnitude of the near-field coefficients can assume huge values for large |n|, values which decrease as N, M, kr are increased. However, it should be borne in mind that the relatively high values of $|E_n^{app} + A_n|$ and $|\mathcal{E}_n^{app} + \mathcal{A}_n|$ do not mean that the incoming wave is not cancelled nor that the total field is divergent for smaller N. The coefficients $|E_n^{app} + A_n|$ and $|\mathcal{E}_n^{app} + \mathcal{A}_n|$ are respectively multiplied by $J_n(k|\mathbf{x}|)$ and $I_n(k|\mathbf{x}|)$ for $\mathbf{x} \in C$ thus for small $k|\mathbf{x}|$ and fixed n the limiting forms $\{J_n(k|\mathbf{x}|), I_n(k|\mathbf{x}|)\} \sim (k|\mathbf{x}|/2)^n/(n!)$ more than compensate for the large values of $|E_n^{app} + A_n|$ and $|\mathcal{E}_n^{app} + \mathcal{A}_n|$ and ensure a reasonable cloaking effect as has already been illustrated qualitatively.

Secondly, it is noted that the near-field effect of cloaking is improved as both M and N are increased, as should be expected and as observed for the far-field coefficients. Fig. 12 indicates that cloaking also improves as kr is increased for fixed values of M, N.

6. Conclusions

The method proposed here gives, in principle, an explicit and precise procedure for cancelling a known incident flexural wave over a finite region of the infinite plate. For plane wave incidence Eqs. (5), (22) and (34)–(36) define the amplitudes of the $M \ge 3$ sources in terms of the incident wave for arbitrary non-dimensional frequency kr and direction of incidence. The analogous amplitudes for point source incidence are discussed (see Eqs. (41), (42)) and it is evident that arbitrary incident flexural wave fields can be accommodated by superposition of these elementary solutions. The active cloaking strategy is based on an expansion of the incident field in cylindrical waves, allowing the source field to be evaluated to any degree of

accuracy by increasing the order of truncation N associated with the number of modes of the sources. Simultaneously the active field is non-radiating because it has been shown that it vanishes identically outside a region \mathcal{R} .

The field cancellation method can be viewed as an inverse problem of finding the source amplitudes required for a given incident wave. Numerical simulations have explored the sensitivity of the derived unique solution to the inverse problem posed. The error associated with an order of truncation N has been studied in some specific scenarios. For both the near- and far-field amplitudes it was shown that the error decreases as N and M increase and as k increases.

In principal the ideas here could be applied to a finite plate with forcing in the time domain, requiring measurements of the incident field at some distance from the cloak region which are then fed back to the active sources in order that they respond accordingly. The solution of the inverse problem is obviously more complicated, but is expected to be unique in the same sense as that derived here. Progress on the finite plate solution requires knowledge of Green's function for flexural vibration in the finite domain, which can be found for specific geometries. However, more realistic structures must account for three dimensional geometry, mode conversion and attenuation [28]. The question of practicality remains open and limitations should be noted associated with the active approach. The sources must be invisible to the incident waves. In practice they themselves would scatter the incident field. Furthermore here it has also been assumed that the Kirchhoff theory holds. In practice a higher-order version of plate theory may be required to properly model the source fields. While Kirchhoff plate theory properly accounts for monopole, i.e. normal force sources, it does not include the effects of localized applied moments [29], which are crucial for modelling multipole sources, whatever their mechanical genesis. Practical implementation must consider the power input into the plate or system by both the desired primary sources and the active secondary sources. Strategies for minimizing the total power in such systems [30] could be useful to consider in conjunction with the present approach.

While the present solution offers, in principle, an exact solution for active cancellation, it depends on exact knowledge of the incident flexural wave field. Limited measurement accuracy must be taken into account in assessing the implementation of active cloaking. Inevitably, the simultaneous constraints of measurement and source fidelity, e.g. number of multipoles, must be balanced. Whatever the outcome, the exact solution of the active cloaking problem given here provides a metric for optimal resolution.

Acknowledgements

Gregory Futhazar thanks the School of Mathematics at the University of Manchester (via the MAPLE Platform Grant (EP/ I01912X/1)) and École doctorale matisse for funding his visit to Manchester in 2013. William J. Parnell is grateful to Rutgers University for financial support for his visit to Andrew Norris in July 2012 when this work was initiated. He is also grateful to the Engineering and Physical Sciences Research Council for funding his research fellowship (EP/L018039/1). Andrew Norris is grateful for support under ONR MURI Grant no. N000141310631.

Appendix A. Modal amplitudes for plane wave incidence

Assuming that the incident wave is a plane-wave of unit amplitude as defined in (33) it follows that with $\mathbf{y} = \mathbf{x}_m + \mathbf{a}_m \in \partial \mathcal{C}_m$, the normal derivative of the displacement is

$$\mathbf{n} \cdot \nabla_{\mathbf{v}} \tilde{\mathbf{w}}(\mathbf{y}) = \mathrm{i} k w_{\mathbf{w}}(\mathbf{x}_{m}) \cos(\theta - \psi) \mathrm{e}^{\mathrm{i} \alpha_{m} \cos(\theta - \psi)}. \tag{A.1}$$

Recalling the definition of $L_{mn}^{ij}(\alpha_m)$ in (37) it is then straightforward to show that

$$\int_{\theta^{(1)}}^{\theta^{(2)}_m} \tilde{w}(\mathbf{y}) e^{-\mathrm{i}n\theta} \, \mathrm{d}\theta = w_{\psi}(\mathbf{x}_m) L_{mn}^{00}(\alpha_m), \tag{A.2}$$

$$\int_{\theta_m^{(1)}}^{\theta_m^{(2)}} \mathbf{n} \cdot \nabla_y \tilde{w}(\mathbf{y}) e^{-in\theta} d\theta = k w_{\psi}(\mathbf{x}_m) L_{mn}^{01}(\alpha_m). \tag{A.3}$$

Noting that $\tilde{\phi}_N(\mathbf{y}) = \mathbf{n} \cdot \nabla_y \tilde{w}(\mathbf{y})$, Eq. (A.3) becomes

$$\int_{\theta_m^{(1)}}^{\theta_m^{(2)}} \tilde{\phi}_N(\mathbf{y}) e^{-in\theta} d\theta = k w_{\psi}(\mathbf{x}_m) L_{mn}^{01}(\alpha_m). \tag{A.4}$$

Furthermore

$$\tilde{\phi}_{T}(\mathbf{y}) = \mathbf{t} \cdot \nabla_{V} \tilde{w}(\mathbf{y}) = -ik w_{w}(\mathbf{x}_{m}) \sin(\theta - \psi) e^{i\alpha_{m} \cos(\theta - \psi)}$$
(A.5)

which yields the result dual to (A.4),

$$\int_{\theta_m^{(1)}}^{\theta_m^{(2)}} \tilde{\phi}_T(\mathbf{y}) e^{-in\theta} d\theta = -ik w_{\psi}(\mathbf{x}_m) L_{mn}^{10}(\alpha_m). \tag{A.6}$$

Moving onto the moment calculations, the normal moment is

$$\tilde{m}_{N}(\mathbf{y}) \equiv \tilde{m}_{ij}(\mathbf{y})n_{i}n_{j} = -D[(1-\nu)\tilde{w}_{,ij}(\mathbf{y})n_{i}n_{j} + \nu\nabla_{y}^{2}\tilde{w}(\mathbf{y})]$$

$$= Dk^{2}w_{\psi}(\mathbf{x}_{m})[(1-\nu)\cos^{2}(\theta-\psi) + \nu]e^{i\alpha_{m}\cos(\theta-\psi)}$$
(A.7)

where the identity $\nabla^2 \tilde{w} = -k^2 \tilde{w}$ has been used. Similarly, the tangential moment is

$$\tilde{m}_{T}(\mathbf{y}) = m_{,ij}(\mathbf{y})n_{i}t_{j} = -D[(1-\nu)\tilde{w}_{,ij}(\mathbf{y})n_{i}t_{j}]
= -Dk^{2}(1-\nu)w_{w}(\mathbf{x}_{m})\sin(\theta-\psi)\cos(\theta-\psi)e^{i\alpha_{m}\cos(\theta-\psi)}.$$
(A.8)

Hence, performing the explicit integration gives

$$\int_{\theta_{m}^{(1)}}^{\theta_{m}^{(2)}} \tilde{m}_{N}(\mathbf{y}) e^{-in\theta} d\theta = -Dk^{2} w_{\psi}(\mathbf{x}_{m})((1-\nu)L_{mn}^{02}(\alpha_{m}) + \nu L_{mn}^{00}(\alpha_{m})),$$

$$\int_{\theta_{m}^{(1)}}^{\theta_{m}^{(2)}} \tilde{m}_{T}(\mathbf{y}) e^{-in\theta} d\theta = iDk^{2}(1-\nu)w_{\psi}(\mathbf{x}_{m})L_{mn}^{11}(\alpha_{m}).$$
(A.9)

These calculations thus provide explicit formulae for the source amplitudes, i.e. (34)–(36). Explicit expressions for the quantities L_{mn}^{ij} are given in the next Appendix.

Appendix B. Evaluation of the integrals defined in (37)

The required quantities L_{mn}^{ij} defined in (37) are determined as follows. Using the Jacobi–Anger identity in the same way as in [15] yields

$$L_{mn}^{00}(\alpha_m) = i^{-n} e^{-in\psi} \sum_{\ell=-\infty}^{\infty} J_{\ell-n}(\alpha_m) F_{\ell}^{(m)}(\psi)$$
(B.1)

where

$$F_{\ell}^{(m)}(\psi) = \begin{cases} \frac{\mathrm{i}^{\ell+1}}{\ell} e^{\mathrm{i}\ell\psi} \left(e^{-\mathrm{i}\ell\theta_m^{(2)}} - e^{-\mathrm{i}\ell\theta_m^{(1)}} \right), & \ell \neq 0, \\ \theta_m^{(2)} - \theta_m^{(1)}, & \ell = 0. \end{cases}$$
(B.2)

On noting that $\frac{\partial L_{mn}^{00}(\alpha)}{\partial \alpha^j} = L_{mn}^{0j}(\alpha)$ it is readily shown that

$$L_{mn}^{0j}(\alpha_m) = i^{-n} e^{-in\psi} \sum_{\ell=-\infty}^{\infty} J_{\ell-n}^{(j)}(\alpha_m) F_{\ell}^{(m)}(\psi)$$
(B.3)

where $J_p^{(j)}(\alpha_m)$ denotes the jth derivative of the Bessel function of order p with respect to its argument α_m . Integration by parts yields explicit expressions for L_{mn}^{10} and L_{mn}^{11} ,

$$\begin{split} L_{mn}^{10}(\alpha_{m}) &= \int_{\theta_{m}^{(1)} - \psi}^{\theta_{m}^{(2)} - \psi} \sin \theta \, e^{i[\alpha_{m} \cos \theta - n(\theta + \psi)]} \, d\theta \\ &= \frac{i}{\alpha_{m}} \left[e^{i[\alpha_{m} \cos \theta - n(\theta + \psi)]} \right]_{\theta_{m}^{(1)} - \psi}^{\theta_{m}^{(2)} - \psi} - \frac{n}{\alpha_{m}} L_{mn}^{00}(\alpha_{m}), \end{split} \tag{B.4}$$

$$\begin{split} L_{mn}^{11}(\alpha_m) &= \mathrm{i} \int_{\theta_m^{(1)} - \psi}^{\theta_m^{(2)} - \psi} \sin \theta \cos \theta \, \mathrm{e}^{\mathrm{i}[\alpha_m \cos \theta - n(\theta + \psi)]} \, \mathrm{d}\theta \\ &= -\frac{1}{\alpha_m} \bigg(\bigg[\cos \theta \mathrm{e}^{\mathrm{i}[\alpha_m \cos \theta - n(\theta + \psi)]} \bigg]_{\theta_m^{(1)} - \psi}^{\theta_m^{(2)} - \psi} + L_{mn}^{10}(\alpha_m) + nL_{mn}^{01}(\alpha_m) \bigg). \end{split} \tag{B.5}$$

Finally, the expression for L_{mn}^{20} follows as

$$L_{mn}^{20}(\alpha_m) = \int_{\theta^{(1)} - y\ell}^{\theta_m^{(2)} - \psi} \sin^2\theta \, e^{i[\alpha_m \cos\theta - n(\theta + \psi)]} \, d\theta = L_{mn}^{00}(\alpha_m) + L_{mn}^{02}(\alpha_m). \tag{B.6}$$

References

- [1] R.J. McKinnell, Active vibration isolation by cancelling bending waves, Proceedings of the Royal Society A 421 (1989) 357–393.
- [2] C.R. Fuller, S.J. Elliott, P.A. Nelson, Active Control of Vibration, Academic Press, London, 1996.
- [3] Harry F. Olson, . Electronic control of noise, vibration, and reverberation, Journal of the Acoustical Society of America 28 (5) (1956) 966.
- [4] A.N. Norris, Acoustic cloaking, Acoustic Today 11 (2015) 38-46.
- [5] U. Leonhardt, Optical conformal mapping, Science 312 (June (5781)) (2006) 1777-1780.

- [6] J.B. Pendry, D. Schurig, D.R. Smith, Controlling electromagnetic fields, Science 312 (5781) (2006) 1780-1782.
- [7] S.A. Cummer, D. Schurig, One path to acoustic cloaking, New Journal of Physics 9 (3) (2007) 45+.
- [8] N. Stenger, M. Wilhelm, M. Wegener, Experiments on elastic cloaking in thin plates, *Physical Review Letters* 108 (January (1)) (2012) 014301+.
- [9] M. Farhat, S. Guenneau, S. Enoch, A.B. Movchan, Cloaking bending waves propagating in thin elastic plates, *Physical Review B* 79 (3) (2009) 033102+.
- [10] D.A. Miller, On perfect cloaking, Optics Express 14 (December (25)) (2006) 12457–12466.
- [11] P.A. Nelson, S.J. Elliott, Active Control of Sound, Academic Press, London, 1992.
- [12] F. Guevara Vasquez, G.W. Milton, D. Onofrei, Active exterior cloaking for the 2D Laplace and Helmholtz equations, *Physical Review Letters* 103 (2009) 073901+.
- [13] F. Guevara Vasquez, G.W. Milton, D. Onofrei, Broadband exterior cloaking, Optics Express 17 (2009) 14800–14805.
- [14] F. Guevara Vasquez, G.W. Milton, D. Onofrei, Exterior cloaking with active sources in two dimensional acoustics, Wave Motion 49 (2011) 515-524.
- [15] A.N. Norris, F.A. Amirkulova, W.J. Parnell, Source amplitudes for active exterior cloaking, *Inverse Problems* 28 (10) (2012) 105002.
- 16] A.N. Norris, F.A. Amirkulova, W.J. Parnell, Active elastodynamic cloaking, Mathematics and Mechanics of Solids 19 (April (6)) (2013) 603–625.
- [17] Y.I. Bobrovnitskii, A new solution to the problem of an acoustically transparent body, Acoustical Physics 50 (November (6)) (2004) 647–650.
- [18] Y. Bobrovnitskii, Impedance acoustic cloaking, New Journal of Physics 12 (2010) 043049+.
- [19] D. Guicking, On the invention of active noise control by Paul Lueg, Journal of the Acoustical Society of America 87 (1990) 2251–2254.
- [20] D. Guicking, Active control of sound and vibration: history, fundamentals, state of the artificial, in: Thomas Kurz, Ulrich Parlitz, Udo Kaatze (Eds.), Oscillations, Waves and Interactions, 60 Years Drittes Physikalisches Institute, Göttingen University, 2007, pp. 107–138.
- [21] A.J. Kempton, The ambiguity of acoustic sources a possibility for active control, Journal of Sound and Vibration 48 (1976) 475-483.
- [22] A. David, S.J. Elliott, Numerical studies of actively generated quiet zones, Applied Acoustics 41 (1994) 63-79.
- [23] G. Futhazar, Ondes en milieux hétérogènes discrets et continus: propagation, diffusion, cloaking, PhD Thesis, Université de Rennes 1 (http://www.theses.fr/2013REN1S149), 2013.
- [24] J. O'Neill, O. Selsil, R.C. McPhedran, A.B. Movchan, N.V. Movchan, Active cloaking of finite defects for flexural waves in elastic plates, ArXiv e-prints, March 2014.
- [25] E. Ventsel, T. Krauthammer, Thin Plates and Shells. Theory, Analysis and Applications, Marcel Dekker AG, Basel, Switzerland, 2001.
- [26] P.A. Martin, Multiple Scattering: Interaction of Time-harmonic Waves with N Obstacles, Cambridge University Press, New York, 2006.
- [27] M. Kitahara, Boundary Integral Equation Methods in Eigenvalue Problems of Elastodynamics and Thin Plates, Elsevier, Amsterdam, 1985.
- [28] L. Cremer, M. Heckl, Björn A.T. Petersson, Structure-Borne Sound: Structural Vibrations and Sound Radiation at Audio Frequencies, 3rd edition, Springer, Berlin, 2005.
- [29] P.W. Smith Jr., C.L. Dym, Input and transfer admittances of thick plates driven by a uniform line moment, *Journal of Sound and Vibration* 60 (1978) 441–447.
- [30] O. Bardou, P. Gardonio, S.J. Elliott, R.J. Pinnington, Active power minimization and power absorption in a plate with force and moment excitation, *Journal of Sound and Vibration* 208 (November (1)) (1997) 111–151.